Agriculture, Ecosystems and Environment 381 (2025) 109435

Contents lists available at ScienceDirect

Agriculture, Ecosystems and Environment

journal homepage: www.elsevier.com/locate/agee

Ecosystem-scale crassulacean acid metabolism (CAM) gas exchange of a sisal (*Agave sisalana*) plantation

Mikko Skogberg [a], Kukka-Maria Kohonen [a,b], Annalea Lohila [a,c], Lutz Merbold [d,e], Matti Räsänen [f], Ilja Vuorinne [g], Petri Pellikka [g,h,i], Timo Vesala [a,f], Angelika Kübert [a,*]

[a] Institute for Atmospheric and Earth System Research / Physics, University of Helsinki, Helsinki, Finland
[b] Institute of Agricultural Sciences, ETH Zürich, Universitätstrasse 2, Zürich 8092, Switzerland
[c] Climate System Research, Finnish Meteorological Institute, Helsinki, Finland
[d] Integrative Agroecology Group, Research Division Agroecology and Environment, Agroscope, Reckenholzstrasse 191, Zürich 8046, Switzerland
[e] Mazingira Centre for Environmental Research and Education, International Livestock Research Institute (ILRI), Naivasha Road, PO 30709, Nairobi 00100, Kenya
[f] Institute for Atmospheric and Earth System Research / Forest Sciences, University of Helsinki, Helsinki, Finland
[g] Department of Geosciences and Geography, University of Helsinki, P.O. Box 64, Helsinki 00014, Finland
[h] State Key Laboratory of Information Engineering in Surveying, Mapping and Remote Sensing, Wuhan University, PR China
[i] Wangari Maathai Institute for Environmental and Peace Studies, University of Nairobi, P.O. Box 29053, Kangemi 00625, Kenya

ARTICLE INFO

Keywords:
Africa
Crop
Soil dryness
Soil moisture deficit
Drought stress
Net ecosystem exchange
Stomatal control
Photosynthetic plasticity
Succulent

ABSTRACT

Plants using crassulacean acid metabolism (CAM) for photosynthesis are particularly adapted to dry conditions, as they can focus on night-time carbon uptake and still exhibit considerable productivity. However, gas exchange measurements of CAM plants at the ecosystem level are scarce. Only a few studies to date report on the carbon dioxide (CO_2) exchange of CAM plants using the eddy covariance (EC) method. We monitored the ecosystem CO_2 exchange of an *Agave sisalana* plantation using the EC method in semi-arid Kenya. Measurements lasted 65 days and began during a wet period that gradually transitioned to a dry period. High productivity periods of *A. sisalana* occurred during the initial wet period with a mean CO_2 uptake of -1.1 μmol m^{-2} s^{-1} (dry period: $+0.3$ μmol m^{-2} s^{-1}). High productivity was related to significant day- and nighttime carbon uptake, indicating direct CO_2 fixation via the C3 pathway during daytime. With decreasing soil moisture, mean daytime net CO_2 exchange became a notable carbon source (from $+1.0$ to $+4.0$ μmol m^{-2} s^{-1}), suggesting a shift of *A. sisalana* towards strict CAM photosynthesis in response to soil drying. Our results demonstrate *A. sisalana*'s high photosynthetic plasticity in relation to soil moisture dynamics and its significance for ecosystem-scale CO_2 fluxes.

1. Introduction

With ongoing global climate change, there is a growing interest on the agricultural potential and growth capacity of crassulacean acid metabolism (CAM) plants in arid regions or otherwise marginal lands. Climate and land-use change are expected to endanger ecosystem services, exacerbate desertification, and land degradation challenges, while changes to land cover are simultaneously driven by increasing populations both in drylands and globally (Smith et al., 2019). In sub-Saharan Africa, agricultural areas increased by 57 % (Brink and Eva, 2009) between 1975 and 2000 due to an intensification of food production. There are hopes of alleviating competing land-use pressures with plants that have adapted specifically to arid environments and can generate yields on traditionally non-arable lands (Borland et al., 2009).

Agaves are succulent plants that are well-adapted to arid conditions and are therefore widely cultivated for agricultural purposes in (semi-) arid regions. Agaves are native in Central America but are grown intensively in vast plantations in South America, Asia, and Africa for plant fiber production (Davis and Ortiz-Cano, 2023). One of their main adaptations is the CAM which is among the three possible photosynthesis pathways. CAM plants close their stomata during the day and collect carbon dioxide (CO_2) during nighttime (Neales et al., 1968; Nobel, 2003; Matiz et al., 2013, 2013), which minimizes water loss through the stomata during daytime. While in the C_3 pathway the carbon is fixed directly by the enzyme Ribulose-1,5-bisphosphate carboxylase/oxygenase (RuBisCO), C_4 and CAM plants have separated the RuBisCO from carbon acquisition; either physically in C_4 plants or temporally in CAM. CO_2 is bound by the enzyme phosphoenolpyruvate

* Corresponding author.
E-mail address: angelika.kuebert@helsinki.fi (A. Kübert).

https://doi.org/10.1016/j.agee.2024.109435
Received 6 August 2024; Received in revised form 7 November 2024; Accepted 8 December 2024
Available online 18 December 2024

carboxylase (PEPC) and stored as malic acid in the plant cells' vacuoles and utilized when there is sunlight. This allows the plants to reduce water loss in harsh environments and reach high water-use efficiencies (Cushman, 2001; Lüttge, 2004; Winter, 2019). During severe drought, gas exchange in CAM plants can even halt altogether because of internal CO_2 storage (Cushman, 2001). Some agaves have been shown to reach high productivities despite the arid and hot environments they often grow in (Garcia-Moya et al., 2011). Not only can they survive drought, but they can also sustain their water use efficiency during dry periods (Ehrler, 1983).

CAM species vary in their level of CAM expression, and some can move within the C_3-CAM spectrum in response to water stress or during plant development (Cushman, 2001). While CAM species generally show large variation in their diurnal gas exchange, agaves are mostly constitutive CAM species, i.e., with nearly fully CAM-typical gas exchange (Winter, 2019). But whether environmental cues alter uptake patterns and photosynthetic mode in CAM species, including agaves, is still unknown (Matiz et al., 2013).

The high productivities that CAM plants can reach are often attributed to direct (daytime) C_3 carbon fixation in well-watered conditions (Winter et al., 2014). Combined day- and nighttime uptake was observed in *Agave tequilana* F.A.C.Weber during periods of maximum CO_2 uptake (Pimienta-Barrios et al., 2001) and wet periods (Owen et al., 2012). *Agave deserti* Engelm. has been reported to shift to mainly daytime uptake under continuous watering (Hartsock and Nobel, 1976). *Agave angustifolia* Haw. has limited photosynthetic plasticity, and around 25 % of total uptake was daytime uptake in well-watered conditions (Winter et al., 2014). In *Agave fourcryodes* Lem., daytime uptake during drought was reduced compared to nighttime uptake, in line with the plant avoiding water loss (Nobel, 1985).

Next to environmental factors, also the plant development can affect the CAM-expression. In young CAM plants, daytime C_3 photosynthesis often accounts for most of the fixed carbon (Winter et al., 2008). In agaves, the fraction of carbon absorbed at night grows with age (Nobel, 2003). Similarly, CAM expression can vary within the plant; in *Agave sisalana* Perrine, for instance, a base-apex gas exchange gradient is present on the leaves. Younger leaf portions closer to the base performed CO_2 uptake almost exclusively during daytime, whereas CAM photosynthesis and nighttime uptake was observed in the more mature leaf tip (J. Hartwell, personal communication in Nobel, 2003).

Gas exchange studies on agaves began in the late 1960s. Early studies on CAM plants were conducted with chambers (Neales et al., 1968). Yet, studies on larger scales, such as with the eddy-covariance (EC) method, are very limited. Measurements of gas exchange in CAM plants and agaves with EC is a new area: San-José et al. (2007) measured *Ananas comosus* (L.) Merr., Jardim et al., (2023) studied *Opuntia stricta* (Haw.) Haw., and Owen et al. (2016) monitored the typical CAM gas exchange pattern of *A. tequilana,* a species closely related to *A. sisalana* (Jiménez-Barron et al., 2020). Both *A. comosus* and *A. tequilana* showed a clear nighttime canopy CO_2 uptake. No nighttime uptake was observed in the *O. stricta* agroecosystem.

However, no EC studies were conducted on *A. sisalana*, a plant of agricultural relevance in Eastern Africa (Stewart, 2015). *A. sisalana* is a perennial xerophyte that grows 200–250 hard, fibrous leaves over several years, after which it blooms and dies. These leaves can grow up to a length of two meters (Lock, 1962). The fiber is commonly used in ropes and twines, composites, baskets, and some textiles, among other things. While the plants tolerate drought well, the optimal annual precipitation for sisal productivity is around 1200 mm (Kimaro et al., 1994). Therefore Stewart (2015) questioned the capability of high sisal productivity relying solely on CAM photosynthesis and called for research into the topic.

In this study, we measured the net ecosystem exchange of CO_2 (NEE) and water vapor (H_2O) over a sisal field in southern Kenya between 23 November 2019 and 26 January 2020 using the EC method. Our main research questions were: (i) How does EC-based CO_2 and H_2O exchange of CAM-dominated vegetation respond to seasonal changes in environmental conditions? (ii) How do environmental conditions alter the diurnal cycle of NEE? (iii) What are the main drivers of NEE in this CAM-dominated agroecosystem? We hypothesized (i) that *A. sisalana* shows a clear CAM-dominated CO_2 exchange, (ii) that CO_2 uptake is larger during the wet season than during the dry season, and (iii) that water is – even though the plant is known to be drought tolerant – a primary driver for CO_2 uptake.

2. Materials and methods

2.1. Measurement setup

2.1.1. Site description and land management

The study was carried out at the Teita sisal estate near Mwatate, Taita Taveta County, Kenya (3°32' S, 38°24' E, Fig. 1). The Teita sisal estate is one of the largest in the world, covering an area of 129.5 km^2 (Wachiye et al., 2021). The most common variety of sisal planted on the estate is *Agave* hybrid 11648, along with *A. sisalana* and *A. sisalana 'hildana'* (Mr Mrombo, personal communication, in: Wachiye et al., 2021). Hybrid 11648 has a longer lifespan than *A. sisalana*, reaching an age of 8–14 years (Wachiye et al., 2021), and higher yields (Kimaro et al., 1994). Bulbils are planted at an age of 1–1.5 years, and 200–250 leaves are cut over the lifecycle of the plant (Carr, 2012). When a plant forms a flower pole, the production of leaves slows down. The plant is then replaced by a new bulbil. As a result, the estate is under constant rotation of different age classes within the blocks. In 2019, sisal plant density on the estate was about 5000 plants ha^{-1}. The leaf biomass, which typically accounts for 85 % of the aboveground biomass in agaves (Corbin et al., 2015, Nobel and Valenzuela, 1987), varied between the blocks from 0 to 47 Mg ha^{-1} with a mean value of 10.6 Mg ha^{-1} (standard deviation: ± 7.10 Mg ha^{-1}). The total sisal biomass of the estate was approximately 94.0 Gg in 2019 (Vuorinne et al., 2021b).

The soils are latosols with poor soil organic carbon content around 1 % (Pellikka et al., 2023).

The primary fertilizer used is sisal residues, applied during planting (Lock, 1962; Wachiye et al., 2021). Other necessary regular management practices on the field include the application of herbicides and pesticides, the removal of stumps and suckers, as well as mowing, grazing and removing bushes of native species. Herbicide was reapplied five days prior to the start of EC measurement to minimize the effect of weeds on ecosystem respiration and primary production.

In Taita Taveta County, rain occurs in a bimodal pattern with long rains occurring approx. between March-May, and short rains in November-December with considerable variations between years. Measurements took place from 23 November 2019 and 26 January 2020 (65 days) and were planned to start from the rainy season and continue to the dry season. Precipitation data from 23 to 30 November 2019 are an average of the precipitation data from the stations Voi (Kenya Meteorological Department, approx. 30 km east) and Maktau (University of Helsinki, approx. 30 km west). Precipitation data from 1 December 2019 to 26 January 2020 are measured in-situ using a tipping bucket rain gauge Campbell ARG100 (Campbell Scientific, Logan, UT, USA).

2.1.2. Eddy covariance setup

The EC system was setup within a 2.6 ha field block growing sisal inside the estate (Fig. 1). The field block had a gentle 5° slope facing to the east and was at an elevation of 840 m above sea level. The location of the EC system was determined according to the prevailing wind direction and local topography so that no topographic barrier was preventing the flow of air. The typical wind direction at the site is east. Measured sisal plants were mature, 5 years old and approximately 1.1 m high. EC measurements were done at 2.60 m height, approximately 1.5 m above the canopy top (Figs. 1B, 1D). Flux footprints (Fig. 1C) were estimated with the FFPonline tool (Kljun et al., 2015). Footprints were short

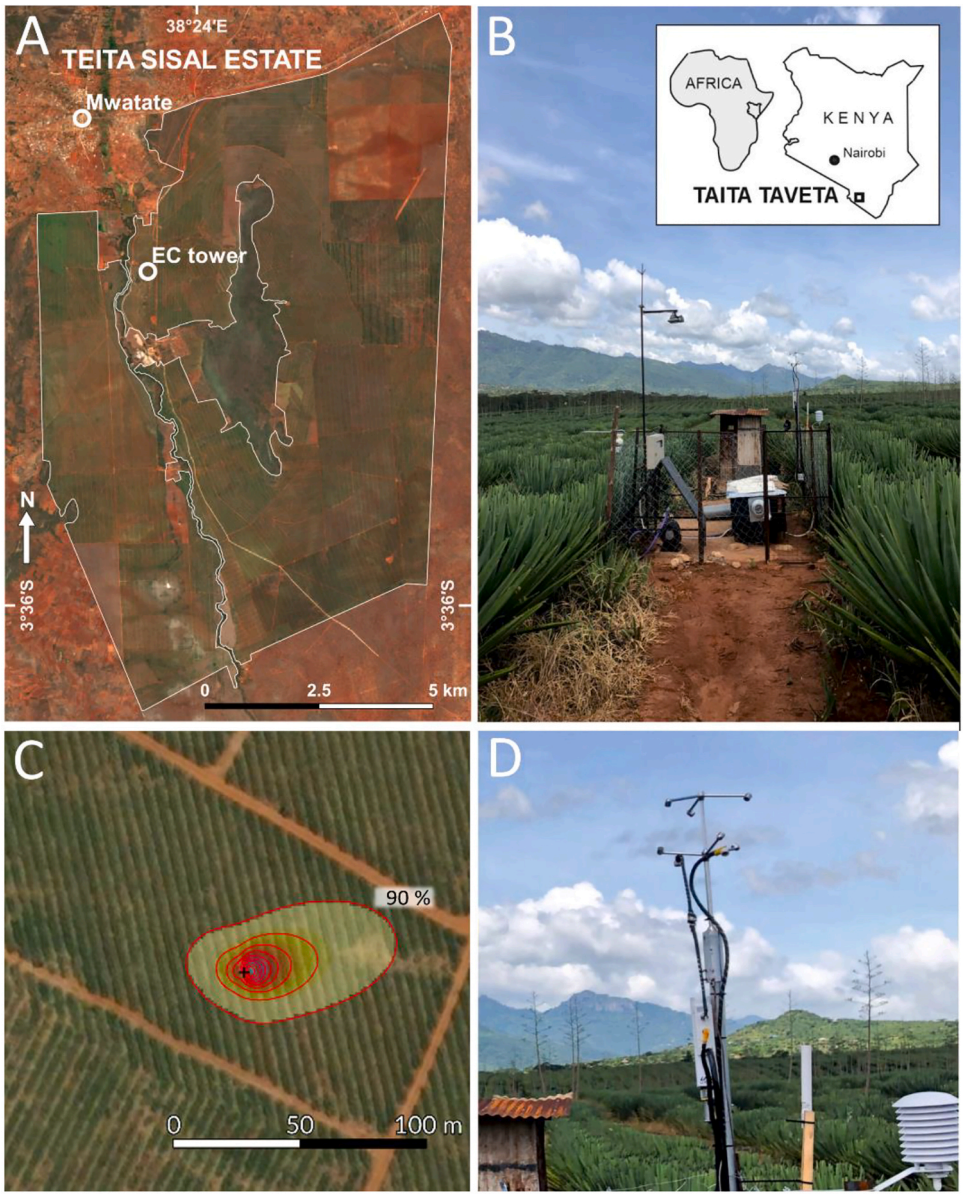

Fig. 1. Teita sisal estate in Taita Taveta County. (A) Location of the eddy covariance (EC) tower within Teita sisal estate (Sentinel-2 satellite image of 28.9.2019). (B) EC tower with Taita Hills in the background, view to the north. (C) EC tower (black cross) in the sisal plot and its flux footprint (red contour lines). Lines represent 90 % of the footprint, shown in 10 % intervals, modelled with FFPonline tool (Kljun et al., 2015). Satellite image: ©2023 Google, CNES/Airbus, Landsat/Copernicus, Maxar Technologies. (D) Gas analyzer inlet tubes and the anemometer are attached to the mast next to the air temperature and moisture sensors. Photographs by P. Pellikka, 2020.

enough that 90 % of the fluxes originated inside the sisal block. An ultrasonic anemometer (USA-1, Metek GmbH, Elmshorn, Germany) measured vertical and horizontal wind components as well as sonic temperature. CO_2 and H_2O mixing ratios were measured with a closed path LI-7200 infrared gas analyzer (LI-COR Inc., Nebraska, USA). All EC measurements were done at 10 Hz sampling frequency.

Meteorological and environmental measurements included net radiation (Kipp & Zonen, Delft, Netherlands), photosynthetic photon flux density (PPFD) (LI-190R quantum sensor, LI-COR Inc., Nebraska, USA), air temperature and relative humidity (Rotronic Instrument Corp., NY, USA). Water vapor pressure deficit (VPD) was calculated from air temperature and relative humidity after Tetens (1930). Soil temperature (Pt100 thermocouples) and soil volumetric water content (Theta Probe ML3, Delta-T Devices, Cambridge, UK) were measured in the upper soil layer (2 cm depth, 0–5 cm). Soil matric potentials were derived from soil volumetric water content using the soil parameters in (see Table 2 in Tuure et al., 2021) and the minimum soil volumetric water content measured at the site as input for the residual water content (6 %-vol). The EC tower was powered by electricity from the sisal estate manager's house approximately 200 m to the south.

2.2. Data processing

30-min EC fluxes were calculated with the software EddyUH (Mammarella et al., 2016) using linear detrending, 2D coordinate rotation, correcting for time lag between sonic anemometer and gas analyzer and correcting for high and low frequency spectral losses (Aubinet et al., 2000; Rannik and Vesala, 1999). Data were quality flagged according to (Mauder et al., 2013) and poor-quality data (flag = 2) was discarded. Nighttime fluxes were filtered for low turbulence using a friction velocity threshold of 0.12 m s^{-1} (Reichstein et al., 2005). Nighttime was defined as time when PPFD < 10 μmol m^{-2} s^{-1} . Technical

reasons accounted for 16 % of EC data missing. Further 30 % of EC data were quality filtered, so that in total 54 % of EC data remained for in-depth data analysis. Negative NEE values indicate uptake of CO_2 from the atmosphere into the ecosystem, positive values indicate release of CO_2 into the atmosphere.

2.3. Data analysis

Based on the topsoil water content (< 10 %-vol, Fig. 2D) and the switch of daytime NEE to primarily positive values (Fig. 2A), we defined the wet period ranging from 23 November to 20 December 2019 (28 days) and the dry period from 21 December to 26 January 2020 (37 days). For each period, we calculated the median of diurnal patterns of NEE, evapotranspiration (ET) and environmental variables considering

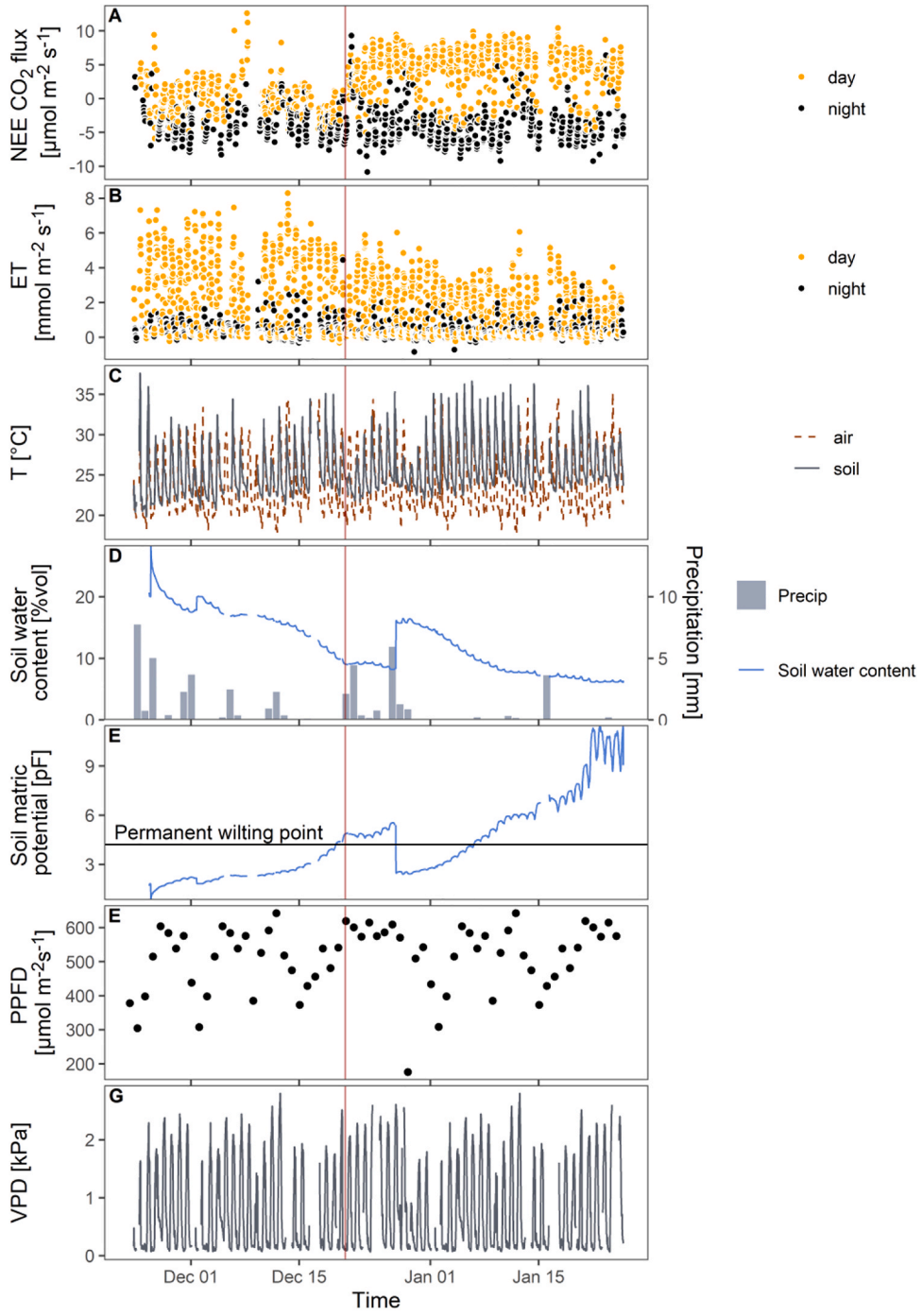

Fig. 2. Time series of **(A)** net ecosystem exchange CO_2 (NEE), **(B)** evapotranspiration (ET), **(C)** air and soil temperature (T; 1.5 m height and 2 cm depth, respectively), **(D)** soil volumetric water content (2 cm depth) and daily precipitation sums, **(E)** soil matric potential (2 cm depth), **(F)** mean daily photosynthetic photon flux density (PPFD) and **(G)** water vapor pressure deficit (VPD). All data are 30-min averages unless otherwise stated and comprise only measured data. NEE and ET are split by day-(orange) and nighttime (black). Negative NEE values indicate uptake of CO_2 from the atmosphere into the ecosystem, positive values indicate release of CO_2 into the atmosphere. Red vertical line indicates the end of the initial wet period and start of a dry period (21 December). Daytime was defined as time when the photosynthetic photon flux density (PPFD) < 10 µmol s^{-1} m^{-2}.

only measured values. For better interpretation, we separated diurnal courses of NEE, ET and environmental variables into four temporal phases: nighttime (phase I, split in Ia (after midnight: 00:00–06:00, and Ib (before midnight: 21:00–00:00)), daytime (III, 09:00–18:00), and the transition phases (II and IV, 06:00–09:00 and 18:00–21:00, respectively), following the four typical CAM phases (Osmond, 1978; Matiz et al., 2013).

Moreover, we analyzed the effect of soil water content on midday measurements (11:00–13:00, measured values) when VPD is high (> 1.5 kPa) and light conditions saturated (PPFD > 500 μmol m^{-2} s^{-1}). We also calculated the canopy conductance g_c as the ratio between ET and mole fraction VPD as in (Cernusak, 2020).

We performed multiple linear regression models for NEE, using environmental variables as predictors variables (air temperature (daily/daytime/nighttime), soil temperature, PPFD, VPD, soil water content, soil matric potential). Also, the previous' days PPFD was included as it can affect the daytime carbohydrate production needed for the nighttime CAM cycle (Owen et al., 2016). Models were calculated for daily/daytime/nighttime means and for 30-minute data, while including for the latter only simultaneous data. We only considered those environmental variables that improved the model's adjusted coefficient of determination (adj. R^2) and root mean square error (RMSE). We also ran daytime mean models that solely included values under light saturation (> 500 μmol m^{-2} s^{-1}) to minimize the effect of PPFD. We tested the collinearity of predictor variables using Variance Inflation Factor (VIF) following (Salmeron et al., 2022).

For analyses of daily/daytime/nighttime and wet/dry period means, data gaps in the 30-min NEE time series were filled using a random-forest model (R package *randomForest*, Liaw and Wiener (2002)). Input parameters for the model were VPD, soil temperature, air temperature, soil moisture, soil matric potentials, and PPFD. The model was trained on a randomly selected data subset (80 %). It was then tested against the test data subset (20 %) for validation (R^2 = 87 % and RMSE = 1.3 $\mu molm^{-2}s^{-1}$). For prediction of NEE, data gaps ≤ 3 hours were filled using linear interpolation. For gaps > 3 hours, we calculated the median value of values ± 2 days at the corresponding time point. Analyses were conducted in Python 3.8 and R version 4.1.2, with the additional R packages *multicoll* (Salmeron et al., 2022) and *randomForest* (Liaw and Wiener, 2002). SD stands for standard variation and IQR for interquartile range.

3. Results

3.1. Environmental variables

Air temperatures during the measurement campaign ranged between 18 °C and 35 °C (Fig. 2C). Mean air temperature was 24 °C, with the daytime/nighttime mean being 27 °C/21 °C. Soil temperatures in the upper soil layer were less variable, with a mean of 26 °C (27 °C/24 °C for day/night). Mean VPD was 0.8 kPa (1.3/0.2 kPa for day/night), with the variation being mostly diurnal (Fig. 2G). Mean maximum PPFD was 1860 (± 520 SD) μmol m^{-2} s^{-1} , with the mean daily value being 510 (± 100 SD) μmol m^{-2} s^{-1} (Fig. 2F).

Rain events occurred at irregular intervals during the 65-day measurement period (Fig. 2D), with a rainfall total of 123 mm over 27 days in the wet period and 103 mm over 38 days in the dry period.

Volumetric soil water content varied between 6 %-vol and 28 %-vol (Fig. 2D). It declined from the beginning of the measurements reaching a low level of less than 10 %-vol around 20 December (red vertical line in Fig. 2). After 21 December, it stayed mostly at lower levels for the rest of the measurements (< 16 %-vol) with only a temporary increase from 8 %-vol to 16 %-vol on 27 December. The mean values before and after 21 December were 17 %-vol and 10 %-vol, respectively. Soil matric potentials (Fig. 2E) dropped below the permanent wilting point (pF 4.2) around 20 December, with a short interruption on 27 December.

Changes in the mean values of other environmental variables between these two periods were small (< 5 %).

3.2. Temporal dynamics of NEE and ET

NEE varied mostly between −10 and + 10 μmol CO_2 m^{-2} $s^{-1}$for the 65 days observation period (Fig. 2A). Mean NEE was −0.3 (± 4.2 SD) μmol m^{-2} s^{-1} , with a median of −0.8 (-3.8 to +2.8 IQR) μmol s^{-1} m^{-2}. The mean daytime NEE was + 2.7 (± 3.2 SD) μmol m^{-2} s^{-1} , whereas the nighttime mean was −3.5 (± 2.3 SD) μmol m^{-2} s^{-1}correspondingly.

While nighttime NEE stayed relatively consistent throughout the time series, daytime activity changed substantially with time. Negative (30-min) values of daytime NEE, indicating uptake of CO_2 from the atmosphere into the ecosystem, were mostly observed during the wet period. On 21 December (left red vertical line, Fig. 2), daytime NEE shifted to higher and primarily positive values. Mean daytime NEE before and after 21 December were + 1.0 and + 4.0 μmol m^{-2} s^{-1} , respectively; mean nighttime NEE were −3.3 and −3.61 μmol m^{-2} s^{-1} , respectively. Mean NEE during the wet and dry period was −1.1 (± 3.1 SD) and + 0.3 (± 4.7 SD) μmol m^{-2} s^{-1} , respectively.

Mean (measured) ET was 1.4 mmol H_2O m^{-2} s^{-1} (2.5/0.3 mmol m^{-2} s^{-1} for day/night; in mm: 25.1/44.6/4.8 for daily/day/night) (Fig. 2B). The mean daytime ET decreased by 41 % when comparing the wet and the dry periods (3.3 and 2.0 mmol m^{-2} s^{-1}, respectively; 59.5 and 35.2 mm, respectively; all values based on measured values).

3.3. Diurnal dynamics of NEE and ET

Diurnal NEE differed notably between the dry and wet period (Fig. 3). During the wet period (Fig. 3A), NEE was lowest early in the night (-2.7 μmol m^{-2} s^{-1}, phase Ia) and rose steadily towards the morning. Around 7:00 in the morning, a pronounced carbon uptake, i.e., a short and sharp reverse in NEE (-0.9 μmol m^{-2} s^{-1}, phase II) occurred. NEE reached highest values around noon (+0.2 μmol m^{-2} s^{-1}, phase III) and started declining in the afternoon (phase IV). Daytime NEE was close to zero, i.e., gross primary production balanced out ecosystem respiration.

In contrast, during the dry period (Fig. 3B), a clear pattern of daytime carbon release and nighttime carbon uptake in NEE was observed. Nighttime NEE (-3.4 μmol m^{-2} s^{-1}, phase Ia) followed a similar uptake pattern as during the wet period. No significant carbon uptake (i.e., short-term NEE decline) was visible in the morning during phase II (+1.6 μmol m^{-2} s^{-1}). NEE reached highest and positive values around noon (+5.4 μmol m^{-2} s^{-1}, phase III) and decreased again in the afternoon (phase IV).

ET showed a similar diurnal pattern for the wet and dry period, with increasing/decreasing ET in response to increasing/decreasing VPD and PPFD. ET was significantly lower during the dry period noon (2.4 mmol m^{-2} s^{-1}, phase III, wet period: 4.2 μmol m^{-2} s^{-1}) (Figs. 3B, 4A).

Midday ET was halved during low soil water content (Fig. 4A). Also, g_c – which accounts for changes in VPD – notably declined with decreasing soil water content (Fig. 4B). Midday NEE was close to zero during the wet period and strongly increased with decreasing soil water content (Fig. 4C).

3.4. Environmental drivers of NEE

VPD, air temperature and PPFD varied mostly diurnal, while soil water content and soil matric potential changed over the course of the measurements. Accordingly, VPD, air temperature and PPFD explained NEE subdaily variation best (all $p < 0.001$, adj. R^2 = 48 %, 46 %, and 44 %, respectively, Fig. S1 and S2, Table S1). Soil water content did not contribute to the variation in subdaily NEE ($p < 0.001$, adj. R^2 = 1 %).

Soil water content had a significant impact on daytime NEE (adj. R^2 = 14 %, $p < 0.001$, 30-min NEE, Fig. S1, Table S1). Most important drivers of daytime NEE were VPD and air temperature (all $p < 0.001$,

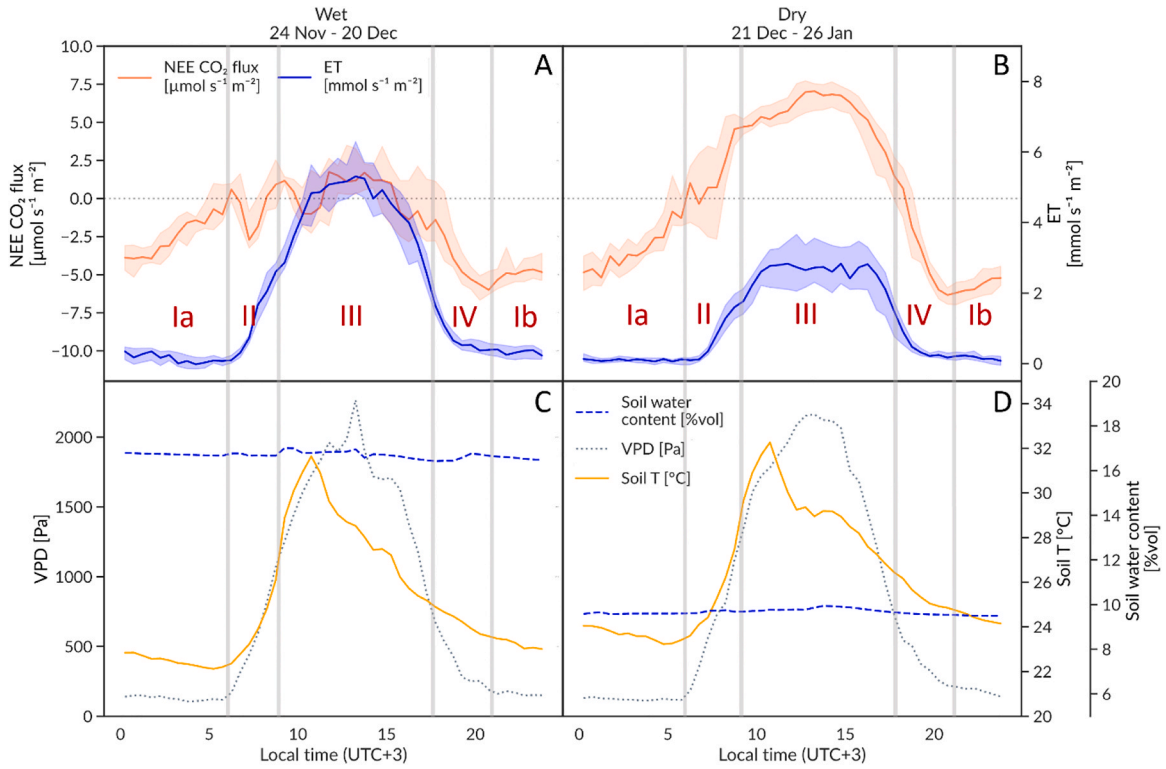

Fig. 3. Diurnal variation of net ecosystem exchange (NEE, red) and evapotranspiration (ET, blue) during the wet period (A) and dry (B) periods. Diurnal variation of soil water content (blue), water vapor pressure deficit (VPD, grey) and soil temperature (orange) during the wet (C) and the dry (D) periods. 30-min medians ± interquartile range (only NEE and ET, measured data). Negative NEE values indicate uptake of CO_2 from the atmosphere into the ecosystem, positive values indicate release of CO_2 into the atmosphere. For better interpretation, the diurnal course was divided into four temporal phases, indicated by grey lines and red roman numerals (I-IV). Phase I was split in Ia (after midnight) and Ib (before midnight).

adj. R^2 = 18 % and 16 %, respectively).

VPD, air temperature and soil water content did not explain nighttime NEE (adj. R^2 = 1 %, 0 % and 7 %, respectively; $p < 0.05$, <0.1, and <0.1, respectively, 30-min NEE, Fig. S1 and S2, Table S1). Nighttime NEE and nighttime soil temperature showed a weak correlation (adj. R^2 = 7 %, $p < 0.001$).

The effect of VPD on subdaily NEE was more pronounced during the dry period (adj. R^2 = 59 %, $p < 0.001$, Table S1) than during the wet period (adj. R^2 = 22 %, $p < 0.001$). Daytime VPD explained 31 % ($p < 0.001$) of daytime NEE during the dry period (wet period: 0 %, non-significant). Accounting for only saturated light conditions, the effect of daytime VPD during the wet and dry periods is 4 % and 27 %, respectively (Fig. 5, $p < 0.01$ and $p < 0.001$, respectively).

Soil water content was the most important driver of daily NEE (20 % $p < 0.001$, Table S2). The mean previous day PPFD did not significantly affect daily NEE (Table S2) nor mean nighttime NEE (Table S3).

VPD and soil water content together explained 50 % of subdaily NEE variation ($p < 0.001$, Table S4). Including soil temperature and PPFD as predictors increased the model's adj. R^2 by 2 % ($p < 0.001$). VPD, soil temperature and PPFD showed a moderate collinearity (VIF = 2.1–4.0). Daytime NEE variation was explained by combined VPD and soil water content by 28 %. Including soil temperature improved the model by 2 % ($p < 0.001$). More statistical results including RMSE values can be found in Table S1-S3.

4. Discussion

The cultivability and growth potential of CAM crops in (semi-)arid environments are receiving increasing attention in face of ongoing climate change. Here, we studied the net CO_2 and H_2O exchange of a sisal plantation in semi-arid Kenya during a transition from a wet to a dry period. Our results show the high photosynthetic plasticity of *A. sisalana* which manifested at the ecosystem level. High productivity and net CO_2 uptake were only observed during the wet period when day- and nighttime carbon fixation occurred. In response to soil dryness, daytime carbon uptake decreased as stomata were closed, turning the sisal agroecosystem to a small carbon source. Net CO_2 dynamics were primarily controlled by changes in primary production of *A. sisalana* as soil CO_2 emissions of the sisal agroecosystem were mostly low, in particular in young to mature stands like the one we investigated (on average between 0.9 and 1.3 µmol m^{-2} s^{-1}, Wachiye et al., 2021). Yet, compared to nearby natural bushlands, soil CO_2 emissions were higher in the sisal blocks, while the estate's aboveground biomass with 11 Mg ha^{-1} was similar to that of nearby bushlands (Vuorinne et al., 2021a, 2021b; Wachiye et al., 2021; Adhikari et al., 2017).

4.1. High carbon uptake through additional daytime uptake during wet period

Daily NEE values were the lowest and carbon uptake of *A. sisalana* the highest during the wet period, when daytime carbon fixation was active (Fig. 2). In young CAM plants, such as the studied *A. sisalana* plants at the Teita sisal estate, the C_3 pathway often accounts for most of the fixed carbon (Winter et al., 2008). High primary production in CAM is often linked to daytime direct C_3 carbon fixation under well-watered conditions (Winter et al., 2014). *A. deserti* was even found to primarily switch to daytime C_3 carbon fixation under continuous watering (Hartsock and Nobel, 1976). *A. tequilana*, on the other hand, used both day- and nighttime fixation to reach high carbon uptake (Pimienta-Barrios et al., 2001). For *A. sisalana*, we also found lowest daily NEE when uptake occurred during the day and night. Consistent nighttime net CO_2 uptake was present throughout the measurements, demonstrating that the ecosystem level gas exchange displayed a clear CAM signal. The nighttime NEE minimum (10 µmol m^{-2} s^{-1}) was similar

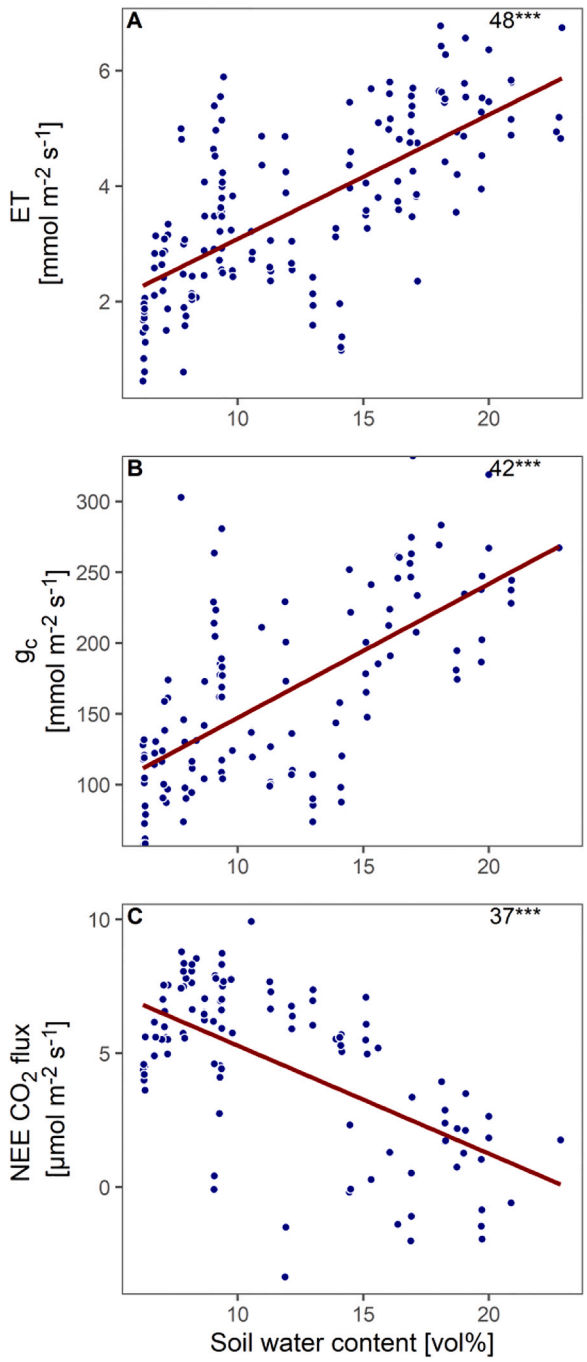

Fig. 4. Midday values (11:00–13:00) under high VPD (> 1.5 kPa) and saturated light (PPFD > 500 µmol m^{-2} s^{-1}) conditions plotted against soil volumetric water content: (A) evapotranspiration ET, (B) canopy conductance g_c and (C) net ecosystem exchange NEE. Negative NEE values indicate uptake, positive values indicate release of CO_2. Numbers indicate the adjusted coefficients of determination (adj. R^2, %) and significance levels (*** < 0.001, ** < 0.01, * < 0.05,. < 0.1). All data are 30-min averages and comprise only measured data.

to the maximum nocturnal (net) uptake reported for *A. fourcryodes* and *A. tequilana* (Garcia-Moya et al., 2011).

4.2. Restriction to nighttime uptake and increased stomatal control during dry period

NEE notably increased with the onset of the dry period (Fig. 2). In response to soil dryness, a clear switch to primarily nighttime carbon uptake was observed. Yet, nighttime uptake of *A. sisalana* remained high despite low soil moisture and soil matric potentials below the permanent wilting point. CAM plants were found to effectively fix carbon even under severe drought (Cushman, 2001). As nighttime uptake did not change from the wet to the dry period, there was likely no upregulation of nighttime carbon uptake as has been observed in some tropical CAM tree species (e.g., Lüttge, 2006; Winter and Holtum, 2007; Winter et al., 2008).

To avoid water loss in the dry period, *A. sisalana* increased its stomatal control, in particular during noon when VPD was high, resulting in decreased carbon uptake. Midday g_c and ET declined notably with decreasing soil moisture and NEE increased (Fig. 4). This behavior was also found for other agaves. *A. fourcryodes*, for instance, reduced its daytime uptake during drought to reduce water loss, but still fixed carbon during night (Nobel, 1985). In addition, stored water in the leaf vacuoles may have postponed the drought response of. *A. sisalana* (Smith et al., 1987, Smith and Winter, 1996, Borland et al., 2011).

Daytime ET losses decreased by 41 % during the dry period, likely due to increased stomatal closure. While transpiration probably contributed a large share to ET in the wet period, soil evaporation likely dominated ET during the dry period. Globally, transpiration seems to control ET (Coenders-Gerrits et al., 2014; Jasechko et al., 2013; Wei et al., 2017). Yet, in semi-arid areas, the contribution of soil evaporation to ET can be high and vary strongly by seasons (Räsänen et al., 2022; Scott et al., 2021; Hu et al., 2009). Räsänen et al. (2022), for instance, reported high transpiration shares from a South-African semi-arid grassland during the wet seasons, contributing up to nearly 100 % to daily ET. In contrast, evaporative losses amounted to up to 90 % of daily ET during the dry seasons.

Interestingly, the rain events and increasing soil water on 27 December did not notably increase daytime carbon uptake, confirming its rather constitutive CAM nature of *A. sisalana* and indicating its switch to the dry season mode. *A. sisalana*'s internal water storages were likely depleted and *A. sisalana*'s may have sensed the start of the dry season.

4.3. Photosynthetic plasticity controls diurnal NEE

The diurnal pattern of NEE differed notably between the dry and the wet period (Fig. 3) and was controlled by *A. sisalana*'s photosynthetic plasticity. In both periods, the highest ecosystem carbon uptake occurred early in the night, which represents CAM phase I (Matiz et al., 2013; Osmond, 1978). In the early morning, when VPD was still low, there was a pronounced uptake (CAM phase II) visible in NEE, yet, significantly stronger during the wet period. CAM phase II was well-captured by the EC system, similar to (Owen et al., 2016) in *A. tequilana*. During the wet period, NEE daytime uptake was likely dominated by direct C_3 carbon fixation, with primary production and ecosystem respiration balancing each other out. In contrast, NEE during the dry period showed CAM-typical daytime release (CAM phase III). In the afternoon, when VPD was lower, stomata typically began to open and NEE declined, corresponding to CAM phase IV (both dry and wet period). This flexible switch between carbon fixing types over the 24-cycle and response to soil water availability demonstrates *A. sisalana*'s remarkable photosynthetic plasticity (Borland and Taybi, 2004).

The patterns in NEE can only indicate the carbon fixing type and the enzyme that were active during carbon uptake. While daytime carbon uptake is likely directly via the enzyme RuBisCO, nighttime uptake occurs through PEPC. However, in some species, daytime carbon uptake during CAM phase III could be still due to PEPC carboxylation. For some species, PECP activation can be extended in the morning, when conditions are still favorable, until the warmest time of the day (e.g., Borland and Griffiths, 1996; Haslam et al., 2002, Winter et al., 2009). For *A. tequilana*, it was found that higher malic acid concentrations can enhance the refixation of CO_2 by Rubisco and decrease the loss of CO_2 during phase III (Borland et al., 2011). Especially succulent species, such as *A. sisalana* and *A. tequilana*, can store large amounts of malic acids in

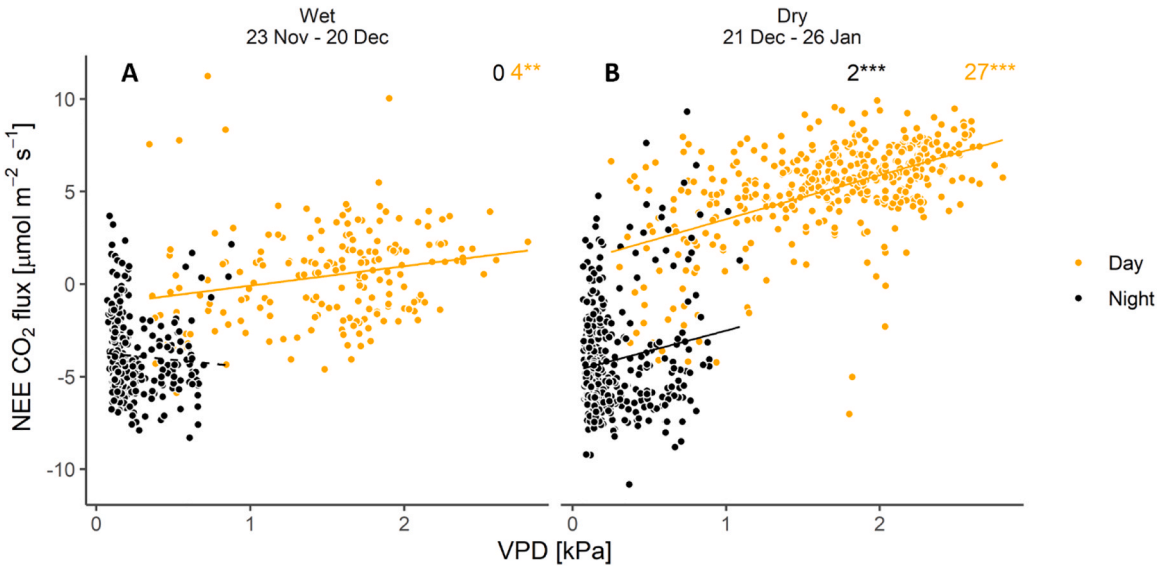

Fig. 5. Relationships between the 30-min net ecosystem CO_2 exchange (NEE) and water vapor pressure deficit (VPD) during the wet (A) and dry (B) periods. Negative NEE values indicate uptake of CO_2 from the atmosphere into the ecosystem, positive values indicate release of CO_2 into the atmosphere. Daytime values include only values under light saturation (PPFD > 500 µmol m^{-2} s^{-1}) and are colored in orange, nighttime values are shown in black. Numbers indicate the adjusted coefficients of determination (adj. R^2, %) and significance levels (*** < 0.001, ** < 0.01, * < 0.05,. < 0.1). All data are 30-min averages and comprise only measured data.

their vacuoles. Nevertheless, the direct fixation of carbon through RuBisCO is more likely as it is more energy efficient than the fixation through PEPC and temporary storage (Winter and Smith, 1996).

4.4. Environmental drivers of NEE

Examining the response of NEE to environmental drivers, we found that VPD – an important driver of stomatal control – had a clear impact on NEE. Subdaily variation in NEE was best explained by VPD which varied mostly diurnal (48 %, $p < 0.001$). Daily VPD did not significantly differ between the wet and the dry period (Figs. 2 and 3). Soil moisture of the upper soil layer, on the other hand, declined significantly during our study period, which altered the effect of VPD on NEE: VPD exerted a stronger control on NEE variation during the dry period (59 %, $p < 0.001$, Table S1) than during the wet period (22 %, $p < 0.001$). *A. sisalana* switched to a strong CAM-typical gas exchange with primarily carbon uptake when VPD was low.

While daytime NEE correlated significantly with VPD and soil water content ($p < 0.001$), neither had a pronounced effect on nighttime NEE (Fig. S1, Table S1). At night, low VPD and thus low transpiration water losses allowed carbon uptake regardless of low soil moisture during the dry period (Fig. 5).

The soil moisture information used here was from the upper 5 cm. Including information from deeper soil depths may further improve the explanation of NEE dynamics. *A. sisalana* has primarily shallow roots but can root down to 50 cm (Abd El Rahman et al., 1967).

For *A. tequilana*, a close relative of *A. sisalana*, Owen et al. (2016) identified nighttime air temperatures and light conditions from the previous day as major drivers of daily NEE variation. While also daily air temperatures and VPD explained NEE to a similar extent, they chose these factors because they were physiologically most relevant. Cooler night temperatures (< 15°C) were found to promote carbon uptake (Owen et al., 2016; Nobel and Valenzuela, 1987). We did not observe this effect here (Table S2), likely because nighttime air temperatures never dropped below 17.9 °C during our study period.

Light conditions can affect the carbon uptake during the following night as sufficient light is needed to fill up the carbohydrate pools required for the nighttime CAM cycle (Borland and Griffiths 1997; Dodd et al., 2003; Borland and Taybi, 2004; Chen and Nose, 2004). We only observed a small effect of the previous day PPFD ($p < 0.05$) on daily NEE and no effect on nighttime NEE (Table S1 and S3). Mean daily PPFD was only below < 200 µmol m^{-2} s^{-1} on one day and light intensities are usually high in these latitudes.

4.5. Growth potential in semi-arid areas

Despite low soil water availability, *A. sisalana* showed still similar nighttime productivity during the dry period as in the wet period. Because of its succulence and CAM-metabolism, it is well-adapted to dry conditions. Yet, these adaptions come at a cost. Succulence reduces the mesophyll conductance, i.e., the conductivity of CO_2 moving from the sub-stomatal cavities to the RuBisCO carboxylation. Compared to the C3 pathway, CAM causes additional metabolic costs of approximately 10 % (Winter and Smith, 1996), which lowers plant productivity. Finally, to give a good estimate of *A. sisalana*'s productivity, our observation period was too short. Our dry-period observations comprised 37 days. Dry conditions in this region can last over several months, such as during the long (natural) dry season, which is usually from April to October. Thus, the productivity of *A. sisalana* may decrease also notably during night with ongoing dry conditions. Owen et al. (2016) studied the gas exchange of in *A. tequilana* – the close relative – for more than 8 months. They found similar productivity in *A. tequilana* as in semi-arid C_3 and C_4 bioenergy crops but with more efficient water use.

Our findings clearly demonstrate that *A. sisalana*'s productivity is the highest during the wet period when both day- and nighttime uptake occur. Other studies also suggested that high productivity of CAM crops, such as *A. comosus* and agaves, are largely because of their high plasticity to use both carbon fixing types. This way, they can increase the duration and the amount of CO_2 uptake over the day (Nobel, 1996; Borland et al., 2009; Holtum et al., 2011, Borland et al. 2011). To confirm this hypothesis, other proxies for stomatal CO_2 uptake, such as carbonyl sulfide flux measurements (Sandoval-Soto et al., 2005), should be tested to partition NEE into gross primary production and ecosystem respiration for CAM-dominated ecosystems.

Previous research found the optimal annual precipitation for sisal productivity was around 1200 mm (Kimaro et al., 1994). Consequently, *A. sisalana* would benefit from additional irrigation, which is particularly problematic for semi-arid regions where increasing rainfall

variability is predicted and land degradation is imminent (Smith et al., 2019; IPCC 2019; Trisos et al., 2022). Considering the expected increasing water scarcity in the future, the productivity of *A. sisalana* may be low (Stewart, 2015; Trisos et al., 2022).

5. Conclusions

Our results clearly show the control of *A. sisalana* on ecosystem CO_2 and H_2O fluxes: its photosynthetic plasticity and response to soil dryness govern the ecosystem net CO_2 and H_2O exchange. Soil water availability limited the productivity of *A. sisalana* and forced a switch to primarily the CAM pathway. While *A. sisalana* can tolerate low soil moistures well, high productivities were only reached during well-watered conditions when both day- and nighttime carbon uptake were possible. *A. sisalana* is a well-adapted crop for semi-arid areas. Yet, semi-arid areas are susceptible to land degradation and, in face of climate change, the productivity of *A. sisalana* and expected crop yields could be low without irrigation. Nevertheless, the cultivation of *A. sisalana* is probably one of the few options to use these marginal lands for sustaining livelihoods.

CRediT authorship contribution statement

Mikko Skogberg: Writing – original draft, Visualization, Validation, Investigation, Formal analysis, Data curation. **Kukka-Maria Kohonen:** Writing – review & editing, Investigation, Data curation. **Annalea Lohila:** Writing – review & editing, Resources, Funding acquisition, Conceptualization. **Lutz Merbold:** Writing – review & editing, Resources, Funding acquisition. **Matti Räsänen:** Writing – review & editing, Resources, Data curation. **Ilja Vuorinne:** Writing – review & editing, Data curation. **Petri Pellikka:** Writing – review & editing, Resources, Project administration, Funding acquisition. **Timo Vesala:** Writing – review & editing, Supervision, Project administration, Funding acquisition, Conceptualization. **Angelika Kübert:** Writing – original draft, Visualization, Validation, Investigation, Formal analysis, Data curation.

Declaration of Competing Interest

The authors declare that they have no known competing financial interests or personal relationships that could have appeared to influence the work reported in this paper.

Acknowledgements

We would like to thank the Teita sisal estate for making it possible for us to conduct the study and for supporting us with the logistics and electricity, without their interest and cooperation the study could not have been done. We thank the staff of Taita Research Station of the University of Helsinki, especially Mwadime Mjomba, for constructing the base for the measurement station as well as helping with the station maintenance and set up, and Muhia Gicheru and Ambrose Nyga for setting up the measurement station. Sami Haapanala is appreciated for setting up the eddy-covariance tower, and George Wanyama from International Livestock Research Institute for assisting with the shipping of instruments. The research was funded by the Academy of Finland for the principal investigators Petri Pellikka and Timo Vesala under the project SMARTLAND (Environmental sensing of ecosystem services for developing climate smart landscape framework to improve food security in East Africa) with project number 318645. Research permit from National Commission for Science, Technology & Innovation of Kenya (P/18/ 97336/26355) is acknowledged. Lutz Merbold acknowledges funding received from the European Union's Horizon Europe Program (grant agreement number 101058525) for the project "Knowledge and climate services from an African observation and Data research Infrastructure (KADI)".

Author contributions

MS and AK wrote the manuscript. PP and TV planned the experiment. KK performed the measurements. LM and MR contributed to the measurement setup. MR and IV provided precipitation data from the stations Voi (Kenya Meteorological Department) and Maktau (University of Helsinki). MS, AK, and KK analyzed the data. AK, TV, and AL led the data analysis and drafted the manuscript. All authors revised the manuscript.

Appendix A. Supporting information

Supplementary data associated with this article can be found in the online version at doi:10.1016/j.agee.2024.109435.

Data availability

Data used in this manuscript are publicly available at https://doi.org/10.5281/zenodo.14445519.

References

Abd El Rahman, A.A., El Gamassy, A.M., Mandour, M.S., 1967. Water economy of agave sisalana under desert conditions. Flora oder Allg. Bot. Ztg. Abt. B, Morphol. und Geobot. 157, 355–378. https://doi.org/10.1016/S0367-1801(17)30081-9.

Adhikari, H., Heiskanen, J., Siljander, M., Maeda, E., Heikinheimo, V., Pellikka, P.K.E., 2017. Determinants of Aboveground Biomass across an Afromontane Landscape Mosaic in Kenya. Remote Sens. 9. https://doi.org/10.3390/rs9080827.

Aubinet M., Rannik U., Snijders W., Valentini, R., Vesala T. 2000. Exchange of Forests: The EUROFLUX Methodology.

Borland, A.M., Griffiths, H., 1996. Variations in the Phases of Crassulacean Acid Metabolism and Regulation of Carboxylation Patterns Determined by Carbon-Isotope-Discrimination Techniques. In: Winter, K., Smith, J.A.C. (Eds.), Crassulacean Acid Metabolism: Biochemistry, Ecophysiology and Evolution, Ecological Studies. Springer, Berlin, Heidelberg, pp. 230–249. https://doi.org/10.1007/978-3-642-79060-7_16.

Borland, A.M., Griffiths, H., 1997. A comparative study on the regulation of C3 and C4 carboxylation processes in the constitutive crassulacean acid metabolism (CAM) plant Kalanchoë daigremontiana and the C3-CAM intermediate Clusia minor. Planta 201, 368–378.

Borland, A.M., Griffiths, H., Hartwell, J., Smith, J.A.C., 2009. Exploiting the potential of plants with crassulacean acid metabolism for bioenergy production on marginal lands. J. Exp. Bot. 60, 2879–2896.

Borland, A.M., Taybi, T., 2004. Synchronization of metabolic processes in plants with Crassulacean acid metabolism. J. Exp. Bot. 55 (400), 1255–1265. https://doi.org/10.1093/jxb/erh105.

Borland, A.M., Zambrano, V.A.B., Ceusters, J., Shorrock, K., 2011. The photosynthetic plasticity of crassulacean acid metabolism: an evolutionary innovation for sustainable productivity in a changing world. N. Phytol. 191, 619–633.

Brink, A.B., Eva, H.D., 2009. Monitoring 25 years of land cover change dynamics in Africa: A sample based remote sensing approach. Appl. Geogr. 29, 501–512. https://doi.org/10.1016/j.apgeog.2008.10.004.

Carr, M.K.V., 2012. Sisal (Ed.). In: Advances in Irrigation Agronomy: Plantation Crops. Cambridge University Press, Cambridge, pp. 187–194 (Ed.).

Cernusak, L.A., 2020. Gas exchange and water-use efficiency in plant canopies. Plant Biol. 22, 52–67.

Chen, L.S., Nose, A., 2004. Day–night changes of energy-rich compounds in crassulacean acid metabolism (CAM) species utilizing hexose and starch. Ann. Bot. 94, 449–455.

Coenders-Gerrits, A.M.J., van der Ent, R.J., Bogaard, T.A., Wang-Erlandsson, L., Hrachowitz, M., Savenije, H.H.G., 2014. Uncertainties in transpiration estimates. Nature 506, E1–E2. https://doi.org/10.1038/nature12925.

Corbin, K.R., Byrt, C.S., Bauer, S., Debolt, S., Chambers, D., Holtum, J.A.M., Karem, G., Henderson, M., Lahnstein, J., Beahan, C.T., Bacic, A., Fincher, G.B., Betts, N.S., Burton, R.A., 2015. Prospecting for energy-rich renewable raw materials: agave leaf case study. PLoS One 10. https://doi.org/10.1371/journal.pone.0135382.

Cushman, J.C., 2001. Crassulacean acid metabolism. a plastic photosynthetic adaptation to arid environments. Plant Physiol. 127, 1439–1448.

Davis, S.C., Ortiz-Cano, H.G., 2023. Lessons from the history of Agave: ecological and cultural context for valuation of CAM. Ann. Bot. 132, 819–833. https://doi.org/10.1093/aob/mcad072.

Dodd, A.N., Griffiths, H., Taybi, T., Cushman, J.C., Borland, A.M., 2003. Integrating diel starch metabolism with the circadian and environmental regulation of crassulacean acid metabolism in Mesembryanthemum crystallinum. Planta 216, 789–797.

Ehrler, W.L., 1983. The transpiration ratios of Agave americana L. and Zea mays L. as affected by soil water potential. J. Arid Environ. 6, 107–113.

Garcia-Moya, E., Romero-Manzanares, A., Nobel, P.S., 2011. Highlights for agave productivity. Glob. Change Biol. Bioengery 3, 4–14.

Hartsock, T.L., Nobel, P.S., 1976. Watering converts a CAM plant to daytime CO 2 uptake. Nature 262, 574–576.

Haslam, R., Borland, A., Griffiths, H., 2002. Short-term plasticity of crassulacean acid metabolism expression in the epiphytic bromeliad Tillandsia usneoides. Funct. Plant Biol. 29, 749–756. https://doi.org/10.1071/pp01214.
Holtum, J.A.M., Chambers, D., Morgan, T., Tan, D.K.Y., 2011. Agave as a biofuel feedstock in Australia. GCB Bioenergy 3, 58–67.
Hu, Z., Yu, G., Zhou, Y., Sun, X., Li, Y., Shi, P., Wang, Y., Song, X., Zheng, Z., Zhang, L., Li, S., 2009. Partitioning of evapotranspiration and its controls in four grassland ecosystems: Application of a two-source model. Agric. For. Meteorol. 149, 1410–1420. https://doi.org/10.1016/j.agrformet.2009.03.014.
IPCC, 2019: Climate Change and Land: an IPCC special report on climate change, desertification, land degradation, sustainable land management, food security, and greenhouse gas fluxes in terrestrial ecosystems [P.R. Shukla, J. Skea, E. Calvo Buendia, V. Masson-Delmotte, H.-O. Pörtner, D. C. Roberts, P. Zhai, R. Slade, S. Connors, R. van Diemen, M. Ferrat, E. Haughey, S. Luz, S. Neogi, M. Pathak, J. Petzold, J. Portugal Pereira, P. Vyas, E. Huntley, K. Kissick, M. Belkacemi, J. Malley, (eds.)]. Cambridge University Press, Cambridge, UK and New York, NY, USA, 896 pp. https://doi.org/10.1017/9781009157988.
Jardim, A.M.R.F., Morais, J.E.F., Jardim, L.S.B., Marin, F.R., Moura, M.S.B., Morellato, L. P.C., Montenegro, A.A.A., Ometto, J.P.H.B., de Lima, J.L.M.P., Dubeux Júnior, J.C. B., Silva, T.G.F., 2023. Sink or carbon source? how the Opuntia cactus agroecosystem interacts in the use of carbon, nutrients and radiation in the Brazilian semi-arid region. J. Hydrol. 625. https://doi.org/10.1016/j.jhydrol.2023.130121.
Jasechko, S., Sharp, Z.D., Gibson, J.J., Birks, S.J., Yi, Y., Fawcett, P.J., 2013. Terrestrial water fluxes dominated by transpiration. Nature 496, 347–350. https://doi.org/10.1038/nature11983.
Jiménez-Barron, O., García-Sandoval, R., Magallón, S., García-Mendoza, A., Nieto-Sotelo, J., Aguirre-Planter, E., Eguiarte, L.E., 2020. Phylogeny, Diversification Rate, and Divergence Time of Agave sensu lato (Asparagaceae), a Group of Recent Origin in the Process of Diversification. Front. Plant Sci. 11, 1651.
Kimaro, D., Msanya, B.M., Takamura, Y., 1994. Review of sisal production and research in Tanzania. Afr. Study Monogr. 15, 227–242.
Kljun, N., Calanca, P., Rotach, M.W., Schmid, H.P., 2015. A simple two-dimensional parameterisation for Flux Footprint Prediction (FFP). Geosci. Model Dev. 8, 3695–3713.
Liaw, A., Wiener, M., 2002. Classification and Regression by randomForest. R. N. 2 (3), 18–22. ⟨https://CRAN.R-project.org/doc/Rnews/⟩.
Lock G.W. 1962. Sisal: twenty-five years' Sisal research. Longmans, Green and Co.
Lüttge, U., 2004. Ecophysiology of crassulacean acid metabolism (CAM). Ann. BOTANY 93, 629–652.
Lüttge, U., 2006. Photosynthetic flexibility and ecophysiological plasticity: questions and lessons from Clusia, the only CAM tree, in the neotropics. New Phytol. 171, 7–25. https://doi.org/10.1111/j.1469-8137.2006.01755.x.
Mammarella, I., Peltola, O., Nordbo, A., Järvi, L., Rannik, Ü., 2016. Quantifying the uncertainty of eddy covariance fluxes due to the use ofdifferent software packages and combinations of processing steps in twocontrasting ecosystems. Atmos. Meas. Tech. 9, 4915–4933. https://doi.org/10.5194/amt-9-4915-2016.
Matiz, A., Mioto, P.T., Mayorga, A.Y., Freschi, L., Mercier, H., 2013. CAM photosynthesis in bromeliads and agaves: what can we learn from these plants? : Photosynth. IntechOpen. https://doi.org/10.5772/56219.
Matiz A., Mioto P.T., Mayorga A.Y., Freschi L., Mercier H. 2013. CAM Photosynthesis in Bromeliads and Agaves: What Can We Learn from These Plants? IntechOpen.
Mauder, M., Cuntz, M., Drüe, C., Graf, A., Rebmann, C., Schmid, H.P., Schmidt, M., Steinbrecher, R., 2013. A strategy for quality and uncertainty assessment of long-term eddy-covariance measurements. Agric. For. Meteorol. 169, 122–135.
Neales, T.F., Patterson, A.A., Hartney, V.J., 1968. Physiological Adaptation to Drought in the Carbon Assimilation and Water Loss of Xerophytes. Nature 219, 469–472.
Nobel, P.S., 1985. Par, Water, and Temperature Limitations on the Productivity of Cultivated Agave fourcroydes (Henequen). J. Appl. Ecol. 22, 157–173.
Nobel, P.S., 1996. High productivity of certain agronomic CAM species. In: Crassulacean acid metabolism: biochemistry, ecophysiology and evolution. Springer Berlin Heidelberg, Berlin, Heidelberg, pp. 255–265.
Nobel P.S. 2003. Environmental Biology of Agaves and Cacti. Cambridge University Press.
Nobel, P.S., Valenzuela, A.G., 1987. Environmental responses and productivity of the CAM plant, Agave tequilana. Agric. For. Meteorol. 39, 319–334. https://doi.org/10.1016/0168-1923(87)90024-4.
Osmond, C.B., 1978. Crassulacean Acid Metabolism: A Curiosity in Context. Annu. Rev. Plant. Physiol. 29, 379–414. https://doi.org/10.1146/annurev.pp.29.060178.002115.
Owen, N.A., Choncubhair, Ó.N., Males, J., Laborde, J.I., del, R., Rubio-Cortés, R., Griffiths, H., Lanigan, G., 2016. Eddy covariance captures four-phase crassulacean acid metabolism (CAM) gas exchange signature in Agave. Plant, Cell Environ. 39, 295–309.
Pellikka, P., Luotamo, M., Sädekoski, N., Hietanen, J., Vuorinne, I., Räsänen, M., Heiskanen, J., Siljander, M., Karhu, K., Klami, A., 2023. Tropical altitudinal gradient soil organic carbon and nitrogen estimation using Specim IQ portable imaging spectrometer. Sci. Total Environ. 883, 163677. https://doi.org/10.1016/j.scitotenv.2023.163677.
Pimienta-Barrios, E., Robles-Murguia, C., Nobel, P.S., 2001. Net CO2Uptake for Agave tequilana in a Warm and a Temperate Environment1. Biotropica 33, 312–318.
Rannik, Ü., Vesala, T., 1999. Autoregressive filtering versus linear detrending in estimation of fluxes by the eddy covariance method. Bound. -Layer. Meteorol. 91, 259–280. https://doi.org/10.1023/A:1001840416858.
Räsänen, M., Aurela, M., Vakkari, V., Beukes, J.P., Tuovinen, J.-P., Van Zyl, P.G., Josipovic, M., Siebert, S.J., Laurila, T., Kulmala, M., Laakso, L., Rinne, J., Oren, R., Katul, G., 2022. The effect of rainfall amount and timing on annual transpiration in a grazed savanna grassland. Hydrol. Earth Syst. Sci. 26, 5773–5791. https://doi.org/10.5194/hess-26-5773-2022.
Reichstein, M., Falge, E., Baldocchi, D., Papale, D., Aubinet, M., Berbigier, P., Bernhofer, C., Buchmann, N., Gilmanov, T., Granier, A., et al., 2005. On the separation of net ecosystem exchange into assimilation and ecosystem respiration: review and improved algorithm. Glob. Change Biol. 11, 1424–1439.
Salmeron, R., Garcia, C.G., Garcia, J., 2022. multiColl: Collinearity Detection in a Multiple Linear Regression Model.
Sandoval-Soto, L., Stanimirov, M., Von Hobe, M., Schmitt, V., Valdes, J., Wild, A., Kesselmeier, J., 2005. Global uptake of carbonyl sulfide (COS) by terrestrial vegetation: Estimates corrected by deposition velocities normalized to the uptake of carbon dioxide (CO 2). Biogeosciences 2 (2), 125–132.
San-José, J., Montes, R., Nikonova, N., 2007. Diurnal patterns of carbon dioxide, water vapor, and energy fluxes in pineapple [Ananas comosus (L.) Merr. cv. Red Spanish] field using eddy covariance. Photosynthetica 45, 370–384.
Scott, R.L., Knowles, J.F., Nelson, J.A., Gentine, P., Li, X., Barron-Gafford, G., Bryant, R., Biederman, J.A., 2021. Water availability impacts on evapotranspiration partitioning, Agriculture. For. Meteorol. 297, 108251. https://doi.org/10.1016/j.agrformet.2020.108251.
Smith, J.A.C., Schulte, P.J., Nobel, P.S., 1987. Water flow and water storage in Agave deserti: osmotic implications of crassulacean acid metabolism. Plant, Cell and Environment 10, 639–648.
Smith, J.A.C., Winter, K., 1996. Taxonomic distribution of crassulacean acid metabolism. In: Lange, O.L., Mooney, H.A. (Eds.), Crassulacean Acid Metabolism: Biochemistry, Ecophysiology, and Evolution. Springer-Verlag, Berlin, pp. 427–436.
Smith P., Campbell D., Cherubini F., Grassi G., Nam V., Lwasa S., McElwee P., Saigusa N., Soussana J.-F., Angel M., et al. 2019. Interlinkages Between Desertification, Land Degradation, Food Security and Greenhouse Gas Fluxes: Synergies, Trade-offs and Integrated Response Options. In: Climate Change and Land: an IPCC special report on climate change, desertification, land degradation, sustainable land management, food security, and greenhouse gas fluxes in terrestrial ecosystems [P.R. Shukla, J. Skea, E. Calvo Buendia, V. Masson-Delmotte, H.- O. Portner, D. C. Roberts, P. Zhai, R. Slade, S. Connors, R. van Diemen, M. Ferrat, E. Haughey, S. Luz, S. Neogi, M. Pathak, J. Petzold, J. Portugal Pereira, P. Vyas, E. Huntley, K. Kissick, M. Belkacemi, J. Malley, (eds.)]. In press.
Stewart, J.R., 2015. Agave as a model CAM crop system for a warming and drying world. Front. Plant Sci. 6, 684.
Tetens, O., 1930. Uber einige meteorologische Begriffe. Z. F. üR. Geophys. 6, 297–309.
Trisos C.H., Adelekan I.O., Totin E., Ayanlade A., Efitre J., Gemeda A., Kalaba K., Lennard C., Masao C., Mgaya Y., Ngaruiya G., Olago D., Simpson N.P., and Zakieldeen S. 2022. Africa. In: Climate Change 2022: Impacts, Adaptation, and Vulnerability. Contribution of Working Group II to the Sixth Assessment Report of the Intergovernmental Panel on Climate Change [H.-O. Pörtner, D.C. Roberts, M. Tignor, E.S. Poloczanska, K. Mintenbeck, A. Alegría, M. Craig, S. Langsdorf, S. Löschke, V. Möller, A. Okem, B. Rama (eds.)]. Cambridge University Press, Cambridge, UK and New York, NY, USA, pp. 1285-1455, doi:10.1017/9781009325844.011.
Tuure, J., Räsänen, M., Hautala, M., Pellikka, P., Mäkelä, P.S.A., Alakukku, L., 2021. Plant residue mulch increases measured and modelled soil moisture content in the effective root zone of maize in semi-arid Kenya. Soil Tillage Res. 209, 104945. https://doi.org/10.1016/j.still.2021.104945.
Vuorinne, I., Heiskanen, J., Maghenda, M., Mwangala, L., Muukkonen, P., Pellikka, P.K. E., 2021a. Allometric models for estimating leaf biomass of sisal in a semi-arid environment in Kenya. Biomass-.-. Bioenergy 155, 106294. https://doi.org/10.1016/j.biombioe.2021.106294.
Vuorinne, I., Heiskanen, J., Pellikka, P.K.E., 2021b. Assessing Leaf Biomass of Agave sisalana Using Sentinel-2 Vegetation Indices. Remote Sens. 13, 233. https://doi.org/10.3390/rs13020233.
Wachiye, S., Merbold, L., Vesala, T., Rinne, J., Leitner, S., Räsänen, M., Vuorinne, I., Heiskanen, J., Pellikka, P., 2021. Soil greenhouse gas emissions from a sisal chronosequence in Kenya. Agric. For. Meteorol. 307, 108465.
Wei, Z., Yoshimura, K., Wang, L., Miralles, D.G., Jasechko, S., Lee, X., 2017. Revisiting the contribution of transpiration to global terrestrial evapotranspiration. Geophys. Res. Lett. 44, 2792–2801. https://doi.org/10.1002/2016GL072235.
Winter, K., 2019. Ecophysiology of constitutive and facultative CAM photosynthesis. J. Exp. Bot. 70, 6495–6508.
Winter, K., Garcia, M., Holtum, J.A.M., 2008. On the nature of facultative and constitutive CAM: environmental and developmental control of CAM expression during early growth of Clusia, Kalanchoë, and Opuntia. J. Exp. Bot. 59, 1829–1840.
Winter, K., Garcia, M., Holtum, J.A.M., 2009. Canopy CO2 exchange of two neotropical tree species exhibiting constitutive and facultative CAM photosynthesis, Clusia rosea and Clusia cylindrica. J. Exp. Bot. 60, 3167–3177.
Winter, K., Garcia, M., Holtum, J.A.M., 2014. Nocturnal versus diurnal CO2 uptake: how flexible is Agave angustifolia? J. Exp. Bot. 65, 3695–3703.
Winter, K., Holtum, J.A.M., 2007. Environment or development? lifetime net CO_2 exchange and control of the expression of crassulacean acid metabolism in *Mesembryanthemum crystallinum*. Plant Physiol. 143 (1), 98–107. https://doi.org/10.1104/pp.106.088922.